Article history
Received: 5th September, 2026
Revised: 14th September, 2026
Accepted: 5th September, 2026
Published: 17th September, 2026

Unicross journal of Science, Engineering & Technology (UJOSET), Journal of the Faculty of Physical Sciences, University of Cross River State
Vol 1 Issue 2, 2026

Article Type: Research

Modelling Redox Kinetics and Trace Metal Dynamics in Waterlogged Agricultural Soils of Biase and Yakurr LGAs of CRS, Nigeria

Kate Asama Effiong*[1], Jeremiah Chukwuebuka Anigbo[1], & Victor Eshu Okpashi[1]

[1]Department of Biochemistry, University of Cross River State, Calabar, Nigeria.
*Correspondence to kate26effiong@gmail.com

Abstract

This study investigated the spatial distribution and redox kinetic dynamics of selected heavy metals in waterlogged agricultural soil in the Yakurr and Biase Local Government Areas of Cross River State, Nigeria. Water samples were collected from twelve farm locations, namely Ekori, Nko, Akpet, Umon, Abini, Agwagune, Mkpani, Idomi, Adim, Ugep, Inyima, and Abaribara. Physicochemical parameters, including pH, temperature, electrical conductivity (EC), total dissolved solids (TDS), and oxidation-reduction potential (ORP), were measured in situ using a Hanna HI98194 multiparameter meter. Heavy metal concentrations were determined by Atomic Absorption Spectrophotometry (PerkinElmer AA Analyst 400) following acid digestion. A first-order redox kinetic model was used to interpret the transformation and mobility of redox-sensitive metals under varying geochemical conditions. The results showed that pH ranged from 6.29 to 6.77, temperature from 26.5 to 32.1°C, EC from 84 to 365 µS/cm, and ORP from 301 to 467 mV. Copper recorded its highest concentration at Umon (0.9970), while nickel was highest at Idomi (1.8397), followed by Ugep (0.9683) and Inyima (0.8714). Arsenic was detected at Idomi, Inyima, Ugep, and Abini, with the highest concentration at Abini (0.1253). Mercury and selenium were not detected in the investigated samples. Idomi, Inyima, and Ugep generally exhibited elevated concentrations of several metals, indicating spatial variability in metal distribution. The redox interpretation suggested that the investigated waterlogged environments were influenced by iron and manganese reduction processes, with implications for trace metal release, retention, and transport. The findings demonstrate that redox conditions, mineral interactions, and site-specific geochemical characteristics contribute to heavy metal behaviour in waterlogged agricultural ecosystems. The study provides baseline information for assessing metal contamination and developing geochemical models to predict metal mobility and environmental risk in the study area.

Keywords: Oxic, Suboxic, Anoxic, waterlogged soil, environmental chemistry, redox kinetics

Cite this article as: Effiong Kate Asama, Anigbo Jeremiah Chukwuebuka, & Victor Eshu Okpashi (2026). Modelling Redox Kinetics and Trace Metal Dynamics in Waterlogged Agricultural Soils of Biase and Yakurr LGAs of CRS, Nigeria. *Unicross Journal of Science, Engineering & Technology* ***1****(2) pp. 77 – 87.*

Introduction

Water bodies and flooded environments undergo rapid changes in their redox conditions when dissolved oxygen becomes depleted following inundation or prolonged water stagnation. As microbial respiration consumes available oxygen, the redox potential (Eh) of the water declines, leading to the sequential utilization of alternative electron acceptors such as nitrate, manganese oxides, iron oxides,

sulfate, and eventually carbon dioxide during methanogenesis (Kelly *et al.*, 2020). These processes are not uniform throughout an aquatic environment but occur across different zones of the water column and at the water-sediment interface, creating strong spatial heterogeneity between oxidized and reduced regions. This heterogeneity strongly influences the solubility, speciation, and transport of trace elements such as Fe, Mn, Cr, Ni, Cu, and Zn (Zhang *et al.*, 2021). Under reducing conditions, the dissolution of Fe and Mn oxides in bottom sediments can release associated trace metals into the overlying water and porewater, significantly increasing their mobility (Yu *et al.*, 2024).

Experimental studies have shown that the duration of flooding and oxygen depletion can control the extent of trace-metal release (Kelly *et al.*, 2020). For example, concentrations of Ni, Cr, and Zn may increase with prolonged oxygen depletion, while Cu may decrease through adsorption or precipitation, and Pb may remain relatively immobile because of its strong association with mineral and particulate phases. Following re-oxygenation, changes in pH and the oxidation of Fe and Mn can immobilize some trace elements through precipitation or adsorption, while others may remain dissolved depending on their affinity for organic matter, suspended particles, and competing ions (Kelly *et al.*, 2020; Campillo-Cora *et al.*, 2021). The kinetics of these redox reactions determine how rapidly oxygen is consumed, how quickly Fe and Mn are reduced, and how rapidly sulfide is produced, thereby playing a crucial role in determining transient peaks in trace-metal mobility (Nwogu *et al.*, 2024). Microbial communities largely mediate these processes, with their activity strongly influenced by the availability of labile organic carbon (Yu *et al.*, 2024). Recent methodological advances have improved the ability to monitor and model aquatic redox dynamics (Yang *et al.*, 2023). Measurements of dissolved oxygen, Eh, pH, electrical conductivity, and trace-element concentrations, combined with sediment and porewater analysis, provide useful information for identifying reducing conditions and determining their duration. When combined with water-column monitoring and electrochemical measurements, these approaches reveal that redox processes can vary considerably over short spatial and temporal scales and may be influenced by water depth, sediment characteristics, organic matter decomposition, hydrological conditions, and biological activity (Sapkota *et al*., 2022).

Waterlogged and stagnant aquatic environments are characterized by prolonged water saturation and restricted oxygen exchange, leading to reducing conditions that drive distinct biogeochemical processes (Hogarth, 2017; Qu *et al*., 2019). Under anoxic conditions, dissolved oxygen is rapidly depleted, forcing microorganisms to utilize alternative electron acceptors such as nitrate, manganese, and iron, which progressively lowers Eh and alters elemental cycling compared with well-aerated waters (Loffredo *et al.*, 2023; Chen *et al.*, 2019). Environmental management practices can also alter redox processes and trace-element dynamics (Glodowska *et al.*, 2020; Okpashi & Abeng, 2020). Organic amendments, for example, can increase microbial activity and oxygen consumption, while materials such as biochar may provide sorption sites and alter pH and microbial redox activity. These effects may immobilize or mobilize trace elements, depending on amendment characteristics, water chemistry, and sediment properties (Qi *et al.*, 2024; Yang *et al.*, 2023). This indicates the need for context-specific evaluation of management practices in aquatic environments. Modelling redox kinetics and trace-element dynamics in tropical areas is therefore important for predicting environmental risks, assessing water quality, supporting sustainable agricultural practices, and informing water-resource management (Nwogu *et al.*, 2024). Therefore, this study aimed to: (1) determine the physicochemical characteristics of water in

selected farmlands in Biase and Yakurr Local Government Areas of Cross River State, Nigeria. (2) quantify the concentrations of redox-sensitive trace elements in the water samples collected from the selected farmlands. (3) Develop a coupled redox-reactive transport model to describe trace element mobilisation and immobilization processes in the waterlogged soils.

Materials and Methods

2.1 Description of Study Area

The research was conducted in the Yakurr and Biase Local Government Areas of Cross River State, Nigeria, a tropical region characterised by high annual rainfall, elevated temperatures, and significant hydrological fluctuations. The study area encompasses twelve sampling locations: Ekori, Adim, Akpet, Umon, Abini, Agwagune, Mkpani, Idomi, Inyima, Ugep, Nko, and Abaribara. The sampling points ranged from 5.24°N to 6.71°N and 7.10°E to 9.44°E, reflecting the region's spatial distribution. These sampling locations comprise agricultural environments influenced by both anthropogenic activities (agricultural practices, potential contamination sources) and natural processes (weathering and organic matter deposition). The tropical climate, presence of organic matter, and spatial variations in oxidation-reduction potential make this area particularly suitable for investigating metal geochemistry in waterlogged ecosystems.

2.2 Sample Collection and Field Measurements

Water samples were collected from twelve different farm locations within the study area to ensure adequate spatial representation. Sampling was conducted using clean, acid-washed containers to minimise contamination and maintain sample integrity for accurate analysis. Field measurements of physicochemical parameters, including pH, temperature, electrical conductivity (EC), total dissolved solids (TDS), and oxidation-reduction potential (ORP), were performed *in situ* using a calibrated multiparameter meter (Hanna Instruments HI98194). These measurements were performed immediately upon sample collection to capture the natural state of the samples without post-collection alteration. We recorded the geographical coordinates of each sampling point (Fig. 1) using a GPS device (Garmin eTrex 10) for documentation, sample identification, and future replication.

2.3 Sample Preparation and Heavy Metal Analysis

Water samples were collected in clean, acid-washed polyethylene bottles and transported to the laboratory for analysis. The samples were thoroughly mixed, and a representative aliquot was measured into a clean digestion flask. The sample was digested using a mixture of hydrochloric acid (HCl) and nitric acid (HNO_3) following standard digestion procedures. The digestion process involved heating the sample-acid mixture gently to reduce the volume and facilitate the breakdown of organic matter, producing a clear solution suitable for heavy metal analysis using Atomic Absorption Spectrophotometry (AAS).

Heavy metal concentrations (Cu, Ni, Zn, Cr, Mn, Fe, Se, Pb, B, V, Mo, Hg, Cd, and As) were determined using an Atomic Absorption Spectrophotometer (PerkinElmer AA Analyst 400). The analytical procedure involved the following steps:

(i) Instrument Calibration: The AAS instrument was calibrated and optimised according to manufacturer specifications for each metal of interest using standard solutions of known concentrations to generate calibration curves with high linearity ($R^2 > 0.995$).

(ii) Sample Analysis: Digested samples were aspirated into the AAS, and absorbance

readings were recorded at specific wavelengths for each metal.

(iii) Quality Control: Analytical quality was assured through the analysis of certified reference materials, reagent blanks, and duplicate samples. Results were expressed as mean ± standard deviation (SD) for triplicate analyses.

2.4 Redox Kinetic Dynamic Model

The Redox Kinetic Dynamic Model was used to investigate the temporal behaviour of redox-active metals in aquatic environments. The model describes the changes in metal concentrations and chemical species as a function of time under specified environmental conditions. It can be used to simulate redox reactions, metal oxidation and reduction, dissolution, precipitation, and the transformation of dissolved metal species under varying geochemical conditions. The model is based on the application of kinetic rate laws and mass balance equations to determine the changes in chemical species over time, whether in a natural water system or a laboratory system.

2.5 Basic First-Order Redox Kinetics Equation

$$\frac{dC}{dt} = -kc$$

where:

i. (C) = concentration of the redox-sensitive species at time (t);
ii. (t) = time;
iii. (k) = first-order reaction rate constant ($time^{-1}$).

The integrated form of the equation is:

$C_t = C_0 e^{-kt}$

where:

i. (C_t) = concentration of the reactant at time (t);
ii. (C_0) = initial concentration;
iii. (k) = first-order reaction rate constant;
iv. (t) = reaction time.

This equation assumes that the rate of transformation is proportional to the concentration of the reacting species. It can be used as an initial approximation for processes such as the depletion of dissolved oxygen or the reduction of specific oxidized species when other reactants are present in excess.

2.6 Data Analysis

Descriptive statistics were calculated for all measured parameters. Metal concentrations were compared with World Health Organisation (WHO) drinking water guidelines to assess regulatory exceedances. Spatial distribution maps were generated using ArcGIS software. Saturation indices were interpreted as follows: SI > 0 indicates supersaturation (precipitation possible), SI = 0 indicates equilibrium, and SI < 0 indicates undersaturation (dissolution favoured).

3.0. Results

3.1. Physicochemical Parameters of Water in the Selected Farm Area

The table shows that the physicochemical properties of water varied across the selected farms. Electrical conductivity ranged from 84 µS/cm in Ugep farm to 365 µS/cm in Ekori farm, while TDS ranged from 46 ppm to 183 ppm, indicating differences in the amount of dissolved substances in the water. The specific gravity was approximately 1.00 in all the samples, showing little variation. The pH values ranged from 6.29 in Nko farm to 6.77 in Abini and Mkpani farms, indicating that the water was generally slightly acidic to near neutral. Temperature ranged from 26.5°C in Nko to 32.1°C in Ugep. ORP values varied from 301 mV in Mkpani and Ekori to 467 mV in Akpet, indicating differences in the oxidation–reduction conditions of the water. PPB and salinity were generally zero or negligible across the farms. Overall, the results indicate moderate variation in water quality characteristics among the farms, particularly in electrical conductivity, TDS, and ORP.

Table 1. Physicochemical Parameters of Waterlogged in Selected Farms of Biase and Yakurr LGAs

Farm	Electrical conductivity µS/CM	Total dissolve solid (TDS) PPM	Specific (sg) Gravity	pH	Temperature ^{0}C	ORD (MV)	PPB	Salt Salinity
Ekori farm	365	174	1.00 at 29.50	6.60	30.9	311	0 at 31.0	0.01 at 3.00
Nko farm	362	183	1.00 at 31.8	6.29	26.5	335	0 at 32.0	0.00 at 31.3
Akpet farm	144	73	1.000 at 31.9	6.54	31.4	467	0. at 31.5	0.00 at 31.5
Umon farm	141	73	1.000 at 31.9	6.54	31.4	410	0 at 31.6	0.00 at 32.6
Abini farm	128	64	1.000 at 32.0	6.77	31.6	310	0 at 32.0	0.00 at 32.4
Agwagune farm	146	74	1.000 at 32.1	6.66	31.6	364	0 at 32.1	0.00 at 32.5
Mkpani farm	86	49	1.000 at 31.6	6.77	31.8	301	0 at 31.6	0.00 at 31.6
Idomi farm	141	64	1.000 at 31.3	6.73	31.7	309	0 at 31.0	0.00 at 31.0
Adim farm	128	64	1.000 at 31.6	6.61	31.7	376	0 at 32.1	0.00 at 32.5
Ugep farm	84	46	1.000 at 31.6	6.70	32.1	336	0 at 31.6	0.00 at 31.6
Inyima farm	132	67	1.000 at 31.7	6.33	31.5	428	0 at 31.3	0.00 at 31.3
Abaribara farm	124	64	1.000 at 31.6	6.61	31.5	371	0 at 32.5	0.00 at 32.5

4.1.2 Heavy Metals and Physicochemical Properties of Water from Selected Farms

Table 1 & 2 shows considerable variation in the heavy metal concentrations and physicochemical properties of water collected from the selected farms. Among the samples, Umon recorded the highest copper (0.9970), while Idomi had a relatively high copper concentration (0.5437). Nickel was highest at Idomi (1.8397), followed by Ugep (0.9683) and Inyima (0.8714). Arsenic was detected mainly in Idomi (0.1191), Inyima (0.0564), Ugep (0.0627), and Abini (0.1253), while mercury and selenium were not detected in any samples. Most of the other metals occurred at relatively low concentrations, although their levels varied considerably among farms. Fluorine showed the greatest concentration at Umon (1.1549) and Adim (1.2511), while Umon also had the highest copper level. The physicochemical results indicate that the water samples were generally slightly acidic to near neutral, with pH values ranging from 6.29 (Nko) to 6.77 (Mkpani and Abini). Electrical conductivity varied substantially, from 84 µS/cm at Ugep to 365 µS/cm at Ekori, suggesting differences in the concentration of dissolved ions among the water sources. Temperatures ranged from 26.5°C at Nko to 32.1°C at Ugep; PPB appears to be zero at each farm location, while oxidation-reduction potential (ORP) ranged from 301 mV at Mkpani to 467 mV at Akpet. Overall, the results demonstrate spatial variation in both heavy metal concentrations and physicochemical characteristics of the farm water sources, with some locations showing comparatively higher metal burdens that may warrant further assessment against relevant drinking-water or irrigation-water standards

Table 2: Heavy Metal concentration of Waterlogged from Selected Farms in Biase and Yakurr LGAs

Farms	Copper (Cu)	Mercury (Hg)	Arsenic (As)	Nickel (Ni)	Zinc (Zn)	Molybdenum (Mo)	Vanadium (V)	Chromium (Cr)	Manganese (Mn)	Selenium (Se)	Boron (B)	Lead (Pb)	Cadmium (Cd)	Fluorine (F)
Idomi	0.5437	ND	0.1191	1.8397	0.1231	0.0033	0.0482	0.2059	0.0404	ND	0.2850	0.0982	0.0304	0.3804
Inyima	0.2575	ND	0.0564	0.8714	0.0583	0.0016	0.0228	0.0976	0.0191	ND	0.1350	0.465	0.0144	0.2621
Ugep	0.2861	ND	0.0627	0.9683	0.0648	0.0017	0.0253	0.1084	0.0213	ND	0.1500	0.0517	0.0160	0.4952
Abaribara	0.0028	ND	ND	0.0091	0.0134	0.0005	ND	0.0040	0.0012	ND	0.0012	0.0016	0.0042	0.2838
Mkpani	0.0056	ND	ND	0.0181	0.0269	0.0010	ND	0.0080	0.0024	ND	0.0025	0.0033	0.0084	0.3575
Abini	0.0061	ND	0.1253	0.0199	0.0295	0.0010	ND	0.0087	0.0026	ND	0.0027	0.0036	0.0093	0.1812
Akpet	0.0040	ND	ND	0.0130	0.0193	0.0007	ND	0.0057	0.0001	ND	0.0018	0.0023	0.0061	0.3986
Nko	0.0051	ND	ND	0.0166	0.0245	0.0009	ND	0.0073	0.0022	ND	0.0023	0.0030	0.0078	0.1425
Ekori	0.0098	ND	ND	0.0314	0.0467	0.0017	ND	0.0138	0.0041	ND	0.0043	0.0057	0.0147	0.2850
Agwagune	0.0056	ND	ND	0.0180	0.0267	0.0009	ND	0.0079	0.0023	ND	0.0025	0.0032	0.0084	0.3128
Umon	0.9970	ND	ND	0.0227	0.0337	0.0012	ND	0.0100	0.0030	ND	0.0031	0.0041	0.0106	1.1549
Adim	0.0035	ND	ND	0.0115	0.0171	0.0006	ND	0.0051	0.0015	ND	0.0016	0.0021	0.0054	1.2511

4.1.3 Spatial Distribution of the Map

This map, as shown in Figure 1, illustrates the spatial distribution of 14 different heavy metals across 11 farming communities in the Yakurr and Biase Local Government Areas of Cross River State, Nigeria. According to the legend, various colored shapes represent specific toxic metals (such as Lead, Mercury, Arsenic, and Cadmium). These markers are densely scattered across the entire mapped region, indicating that heavy metal presence is widespread rather than isolated. The study area is connected by a network of major and minor roads, with several rivers and streams traversing the land, particularly near communities like Abini and Akpet. Because this is a study of farm communities, the ubiquitous presence of these metals poses significant environmental and health risks, potentially threatening local soil quality, water sources, and food safety. In short, the map serves as a critical environmental baseline, identifying pollution hotspots to guide future agricultural safety assessments and remediation efforts in the region

.

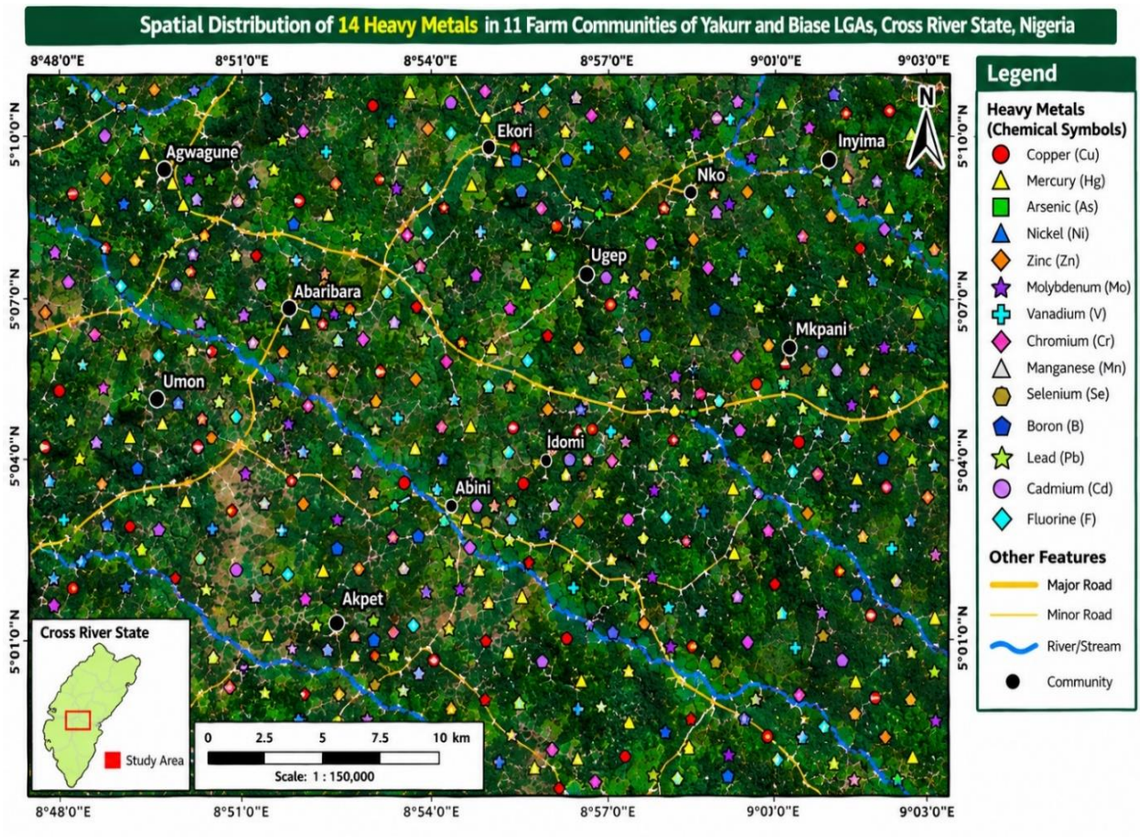

Figure 1, Spatial Distribution of the Map

4

.1. Redox Kinetic Dynamic Model

The Table below shows measured Eh values (301–467 mV) that definitively position the waterlogged environment within the ferric/manganic reduction window. In accordance with the Gibbs free energy yield (ΔG°) of standard redox half-reactions, Mn (IV) → Mn (II) is the most energetically favourable TEAP at this Eh; however, the ubiquitous low Mn concentrations (< 0.04 mg/L) reveal that Mn-oxides are not the rate-limiting electron acceptors; they are simply scarce. Consequently, Fe (III) (hydr)oxide reduction becomes the primary sink for electrons, as evidenced by the pervasive detection of dissolved Fe^{2+} across all farms. The waterlogged ecosystem functions as a dynamic redox boundary, where Fe-oxide reduction is the principal kinetic engine driving trace metal mobility, yet anomalous site-specific mineralogy (Mn-rich phases or organic Cu-complexes) can introduce accelerated kinetic pathways that deviate from the classical thermodynamic sequence.

Discussion

The distribution of metals among the investigated waterlogged farms showed considerable spatial variability, with Idomi, Inyima and Ugep generally recording higher concentrations than the other locations. At Idomi, Cu, As, Ni, Zn, Mo, V, Cr, Mn and Pb were detected at 0.5437, 0.1191, 1.8397, 0.1231, 0.0033, 0.0482, 0.2059, 0.0404 and 0.2850, respectively. Inyima and Ugep also recorded relatively elevated concentrations of several metals, whereas Abaribara, Mkpani, Akpet, Nko, Ekori, Agwagune and Adim generally had lower concentrations. Mercury, selenium and boron were not detected across the investigated locations.

The observed spatial variability is consistent with previous studies showing that trace-metal distribution in flooded soils is influenced by differences in soil mineralogy, pH, redox potential, organic matter, and hydrological conditions (Rinklebe *et al*. 2020). Okpashi (2024) explained that flooding can alter metal mobility through changes in pH, dissolved organic matter, Fe/Mn oxide dissolution, and sulphate reduction. Similarly, Du Laing *et al*. (2009) reported that the spatial occurrence of processes affecting metal mobility in floodplain soils is influenced by topography and changing redox conditions. These studies support the interpretation that the relatively elevated metal concentrations at Idomi, Inyima, and Ugep may reflect differences in geochemical conditions and metal retention capacity rather than a uniform distribution across the investigated farms. Nickel showed a particularly strong spatial pattern. Its concentration reached 1.8397 at Idomi, compared with 0.8714 at Inyima and 0.9683 at

Ugep, while most other farms recorded substantially lower values. This variation suggests differences in mineral sources, adsorption capacity or waterlogging-related release (Huang *et al*., 2023). Reduction of Fe and Mn minerals may decrease available adsorption surfaces, allowing previously retained metals such as Ni to enter the soil solution.

Table 3: Redox Kinetic Dynamic Model

Kinetic Parameter	Observed Metrics / Range	Inferred Redox Kinetics & Thermodynamic State
System Thermodynamic Drive (Eh/pH)	Eh (ORP) = 301 – 467 mV; pH = 6.29 – 6.77 (avg. 6.55).	The positive Eh places the system in the suboxic/manganic-ferric transition zone. Thermodynamic sequencing predicts Mn (IV) reduction initiates first, followed closely by Fe (III) reduction. Sulfate reduction (Eh < -100 mV) and methanogenesis are thermodynamically prohibited.
Mn(IV)-Reduction Kinetics	$[Mn^{2+}]$ = 0.0012 – 0.0404 mg/L (uniformly low across all farms).	Despite being thermodynamically favourable under these Eh/pH conditions, the kinetic flux is severely limited by the low abundance of solid-phase Mn oxide. The reaction is substrate-controlled, exhibiting zero-order-like limitation relative to electron donors.
Fe(III)-Reduction Kinetics	$[Fe^{2+}]$ = 0.1425 – 1.2511 mg/L; Highest at Adim (1.251) and Umon (1.155).	Fe reduction is the dominant terminal electron-accepting process (TEAP). However, kinetics vary spatially: Adim/Umon show high dissolved Fe^{2+} despite moderate Eh (376–410 mV), indicating localized microsite accumulation or rapid ligand-promoted dissolution. In contrast, Idomi/Ugep (Eh ~309–336 mV) exhibit moderate Fe^{2+} (0.38–0.50 mg/L), suggesting steady-state removal via re-adsorption or precipitation.
Trace Metal (Cu, Zn, Pb, Cd) Release Kinetics	Highest total load in Idomi (Cu=0.5437; Zn=0.1231), Ugep (Cu=0.2861; Zn=0.0648), and Umon (Cu=0.9970).	Metal release is kinetically coupled to Fe/Mn-oxide reductive dissolution. The rate of metal desorption follows a first-order dependency on Fe reduction for Idomi/Ugep. Umon is a clear kinetic outlier: extremely high Cu (0.997) at high Eh (410 mV) suggests a separate, faster kinetic pool (e.g., colloidal organic-Cu complexes or direct ion-exchange) operating independently of reductive dissolution.
Arsenic (As) Mobilization Kinetics	Detected only in Idomi (0.1191), Inyima (0.0564), Ugep (0.0627), and Abini (0.1253).	As release is partially decoupled from Fe. While Idomi/Ugep follow the expected co-release with Fe, Abini presents a kinetic anomaly: high As (0.125) with low Fe (0.181). This indicates that As is preferentially released via rapid reductive desorption from Mn-oxides or a highly labile surface complex, exhibiting a faster initial kinetic rate constant compared to bulk Fe-oxide reduction.
Critical Kinetic Threshold (ORP)	ORP < ~350 mV (e.g., Idomi 309, Mkpani 301, Ugep 336).	Below this threshold, the rate of Fe(III) reduction accelerates exponentially, driving a significant increase in the dissolved pool of redox-sensitive metals (Cu, Zn, Pb, Cd, As). Above 400 mV, the system is kinetically "buffered" by Mn cycling, limiting trace metal flux.

Arsenic, chromium and manganese also showed important redox-related patterns. Arsenic was detected at Idomi, Inyima, Ugep and Abini. Under reducing conditions, Fe (III) reduction can dissolve Fe minerals that retain arsenic, while As (V) may be transformed to the more mobile As (III) form. Chromium also varied considerably, with the highest value at Idomi. However, because total chromium was measured, the individual contributions of Cr (III) and Cr (VI) cannot be established Okpashi (2024). Manganese, a strongly redox-sensitive

element, was highest at Idomi, followed by Inyima and Ugep, reflecting its potential usefulness as an indicator of reduction processes (Zhang *et al*., 2024). Lead and zinc were also strongly site-dependent. Their mobility may be influenced indirectly by Fe/Mn oxide dissolution, adsorption, organic complexation and, under strongly reducing conditions, sulfide precipitation. Overall, the spatial patterns demonstrate that metal behaviour is closely connected with redox conditions and mineral interactions. These findings provide a useful basis for modelling metal transport using coupled redox, sorption and precipitation processes
.

Conclusion

The findings demonstrate considerable spatial variability in the distribution of redox-active and redox-associated metals across the investigated waterlogged farms, with Idomi, Inyima and Ugep emerging as the major metal-enriched locations. The pronounced concentrations of Ni, Zn, Cu, As, Cr, Mn and Pb at these sites indicate that local geochemical conditions, mineral composition and possible site-specific sources strongly influence metal accumulation and mobility. The correlation results further show that redox conditions are particularly important for As, which exhibited strong negative relationships with ORP, suggesting that increasingly reducing conditions may enhance its mobility under waterlogged conditions. The results confirm that metal behaviour in waterlogged soils is controlled by interconnected redox, pH, mineral dissolution, sorption, complexation and precipitation processes rather than by concentration alone. Metals such as As, Mn, Cr, and Mo show direct or strong redox-related behaviour, whereas Cu, Ni, Zn, and Pb are better considered redox-coupled through interactions with Fe and Mn oxides and sulphide minerals. The non-detection of Hg and Se indicates concentrations below the analytical detection limits, not complete absence. Therefore, the observed spatial patterns provide a strong basis for developing redox kinetics and transport models capable of predicting metal release, retention, and mobility under changing waterlogged and redox conditions. Such modelling, supported by species-specific measurements and site-specific kinetic parameters, will improve understanding of metal bioavailability and potential risks to rice production and food safety in the studied farms.

Conflict of interest: No conflict of interest

AI disclosure: This article was researched and drafted with the assistance of artificial intelligence. While AI generated initial concepts and structure, a human author thoroughly reviewed, fact-checked, and edited the final content to ensure accuracy, originality, and adherence to our editorial standards

Funding: Not applicable.

Data Availability: The data supporting these findings are contained in this article and can be made available from the corresponding author upon request.

Authors' Contribution: All authors contributed equally.

References

Campillo-Cora, C., Soto-Gómez, D., Arias-Estévez, M., Bååth, E., & Fernández-Calviño, D. (2021). Bacterial community tolerance to Cu in soils with geochemical baseline concentrations (GBCs) of heavy metals: Importance for pollution-induced community tolerance (PICT) determinations using the leucine incorporation method. Soil Biology and Biochemistry, 155, 108157. https://doi.org/10.1016/j.soilbio.2021.108157

Chen, C., Li, L., Huang, K., Zhang, J., Xie, W.-Y., Lu, Y., Dong, X., & Zhao, F.-J. (2019). Sulfate-reducing bacteria and methanogens are involved in arsenic methylation and demethylation in paddy soils. The ISME Journal, 13(10), 2523–2535. https://doi.org/10.1038/s41396-019-0451-7

Du Laing, G., Rinklebe, J., Vandecasteele, B., Meers, E., & Tack, F. M. G. (2009). Trace metal behaviour in estuarine and riverine floodplain soils and sediments: A review. *Science of the Total Environment*, *407*(13), 3972–3985. https://doi.org/10.1016/j.scitotenv.2008.07.025

Glodowska, M., Stopelli, E., Schneider, M., Rathi, B., Straub, D., Lightfoot, A., Kipfer, R., Berg, M., Jetten, M., Kleindienst, S., & AdvectAs Team Members. (2020). Arsenic mobilization by anaerobic iron-dependent methane oxidation. Communications Earth & Environment, 1, 42. https://doi.org/10.1038/s43247-020-00037-y

Hogarth, P. J. (2017). Waterlogging and soil redox processes. In Soil biochemistry and ecology (pp. 45–76). Academic Press.

Huang, K., Yang, Y., Lu, H., Hu, S., Chen, G., Du, Y., Liu, T., Li, X., & Li, F. (2023). Transformation kinetics of exogenous nickel in a paddy soil during anoxic-oxic alteration: Roles of organic matter and iron oxides. Journal of Hazardous Materials, 452, 131246. https://doi.org/10.1016/j.jhazmat.2023.131246

Kelly, T. J., Hamilton, E., Watts, M. J., Ponting, J., & Sizmur, T. (2020). The effect of flooding and drainage duration on the release of trace elements from floodplain soils. *Environmental Toxicology and Chemistry*, *39*(11), 2124–2135. https://doi.org/10.1002/etc.4830

Loffredo, J. A., Rabenhorst, M. C., Stolt, M. H., & Amador, J. A. (2023). Potential interference of organic acids and ferrous iron in the interpretation of Fe and Mn indicators of reduction in soil. Soil Science Society of America Journal, 87(5), 1165–1173. https://doi.org/10.1002/saj2.20560

Nwogu, F. U., Nwajiobi, B., Ogbonna, A. N., & Ubuoh, E. A. (2024). Soil quality dynamics and degradation potentials as influenced by land use systems in humid tropical soil of Southeastern Nigeria. Journal of Agriculture and Environment,19(2),277–304. https://doi.org/10.4314/jagrenv.v19i2.25

Okpashi, V.E. (2024). Estimation Of Redox-Sensitive Metals in Lafarge Cement Company's Area in Akamkpa, Nigeria: Assessment of Ecological Health Risk, *Science World Journal* Vol. 19(No 1), https://dx.doi.org/10.4314/swj.v19i1.27

Okpashi, V.E. (2024). Source Generation of Arsenic Species and Spatial Distribution in Benthic Ecosystems: A Review. In: Kumar, N., Hashmi, M.Z., Wang, S. (eds.), Arsenic Toxicity Remediation. Emerging Contaminants and Associated Treatment Technologies. *Springer, Cham*. https://doi.org/10.1007/978-3-031-52614-5_4.

Okpashi, V.E., and Abeng, F.E. (2020). Predicting the Outcome of Arsenic Toxicity on Exposed Juvenile Male Humans: A Shift to Infertility. Book chapter in a book titled "Arsenic toxicity: Challenges and solutions". *Publisher: Springer Nature*. Pp. 1 - 26. https://www.springer.com/gp/book/9789813360679.

Qi, S., Degen, A., Wang, W., Huang, M., Li, D., Luo, B., Xu, J., Dang, Z., Guo, R., & Shang, Z. (2024). Systematic review for the use of biochar to mitigate soil degradation. GCB Bioenergy, 16(6), e13147. https://doi.org/10.1111/gcbb.13147

Qu, C., Chen, W., Hu, X., Cai, P., Chen, C., Yu, X.-Y., & Huang, Q. (2019). Heavy metal behaviour at mineral-organo interfaces: Mechanisms, modelling and influence factors. Environment International, 131, 104995. ttps://doi.org/10.1016/j.envint.2019.104995

Rinklebe, J., Antoniadis, V., Shaheen, S. M., Rosche, O., & Altermann, M. (2019). Health risk assessment of potentially toxic elements in soils along the Central Elbe River, Germany. *Environment International*, *126*, 76–88. https://doi.org/10.1016/j.envint.2019.02.011

Sapkota, Y., Duball, C., Vaughan, K., Rabenhorst, M. C., & Berkowitz, J. F. (2022). Indicator of reduction in soil (IRIS) devices: A review. Science of the Total Environment, 852, 158419. https://doi.org/10.1016/j.scitotenv.2022.158419

Yang, X., Wen, E., Ge, C., El-Naggar, A., Yu, H., Wang, S., Kwon, E. E., Song, H., Shaheen, S. M., Wang, H., & Rinklebe, J. (2023). Iron-modified phosphorus- and silicon-based biochars exhibited various influences on arsenic, cadmium and lead accumulation in rice and enzyme activities in a paddy soil. Journal of Hazardous Materials, 459, 132172. https://doi.org/10.1016/j.jhazmat.2023.132172

Yu, Q., Wen, J., Zhang, S., Wu, C., Ouyang, H., Hu, N., Li, X., & Qiu, X. (2024). The coupling of sulfide and Fe-Mn minerals promotes the migration of lead and zinc in the redox cycle of high pH floodplain soils. Journal of Hazardous Materials, 472, 134546. https://doi.org/10.1016/j.jhazmat.2024.134546

Zhang, X., Zhang, P., Wei, X., Peng, H., Hu, L., & Zhu, X. (2024). Migration, transformation of arsenic, and pollution control strategies in paddy soil-rice system: A comprehensive review. Science of the Total Environment, 951, 175500. https://doi.org/10.1016/j.scitotenv.2024.175500

Zhang, Z., Guo, G., Zhao, H., Wu, D., Zhang, Y., Li, X., & Wang, Y. (2021). Partitioning, leachability, and speciation of chromium in the size fractions of soil contaminated by chromate production. Chemosphere, 263, 128308. https://doi.org/10.1016/j.chemosphere.2020.128308